# New self-consistent model of daytime emissions of $O_2(a^1\Delta_g,\ v \geq 0)$ and $O_2(b^1\Sigma_g^+,\ v = 0, 1, 2)$ in the middle atmosphere. Retrieval of vertical ozone profile from the measured intensity profiles of these emissions

**V.A. Yankovskii and R.O. Manuilova**

*V.A. Fok Research & Development Institute of Physics, St. Petersburg State University, Petrodvorets*

Received November 22, 2002

Traditional kinetics of electronically excited products of $O_3$ and $O_2$ photolysis is supplemented with the processes of energy transfer between vibrational-electronic excited states of the $O_2$ molecule $O_2(a^1\Delta_g,\ v \geq 1)$ and $O_2(b^1\Sigma_g^+,\ v \geq 1)$ and the $O_2$ molecule in the ground state $O_2(X^3\Sigma_g^-,\ v \geq 1)$. The model proposed allows calculating not only the vertical profiles of the $O_2(a^1\Delta_g,\ v = 0)$ and $O_2(b^1\Sigma_g^+, v = 0)$ concentrations, but also the profiles of $[O_2(a^1\Delta_g, v = 1–5)]$ and $[O_2(b^1\Sigma_g^+,\ v = 0, 1, 2)]$. When vibrational-electronic kinetics of excited products of ozone and oxygen photolysis is taken into account, the ozone concentration profiles retrieved separately from measured intensities of 762 nm and 1.27 μm emissions turn out to be in a good agreement.

## Introduction

One of the methods to determine the ozone concentration in the middle atmosphere is monitoring of $O_2$ emissions in the atmospheric band:

$$O_2(b^1\Sigma_g^+, v = 0) \rightarrow O_2(X^3\Sigma_g^-,\ v = 0) + \text{photon}\ (\lambda = 762\ \text{nm})$$

and in the IR atmospheric band:

$$O_2(a^1\Delta_g,\ v = 0) \rightarrow O_2(X^3\Sigma_g^-, v = 0) + \text{photon}\ (\lambda = 1.27\ \mu\text{m}).$$

For brevity, these bands will be denoted below as Atm (0, 0) $O_2$ and IR Atm (0, 0) $O_2$, respectively.

Electronically excited oxygen molecules can be generated through three processes:

1) at ozone photolysis,

2) as a result of energy redistribution at collisions of oxygen molecules with the excited products of $O_2$ and $O_3$ photolysis,

3) at the absorption of solar radiation in Atm (0, 0) and IR Atm (0, 0) bands of $O_2$.

As the ozone absorbs solar radiation within the Hartley band, singlet energy states of oxygen molecules $O_2(a^1\Delta_g)$ and atoms $O(^1D)$ are generated. Another source of $O(^1D)$ atoms is photolysis of $O_2$ in the Schumann–Runge continuum (SRC). Energy transfer from $O(^1D)$ to oxygen molecules along with the absorption of solar radiation in the 762 nm band leads to populating the second excited singlet level $^1\Sigma_g^+$ of the $O_2$ molecule.[1,2,3] Then in the collisional processes the energy is transferred from $O_2(b^1\Sigma_g^+,\ v = 0)$ to $O_2(a^1\Delta_g)$. An additional source of $O_2(a^1\Delta_g)$ is the absorption of solar radiation by the $O_2$ molecules in the 1.27 μm band.[3] Knowing the mechanism of population of the $O_2$ singlet levels, it is possible to retrieve the ozone concentration from observations of the emissions within the above-mentioned bands.[1,4] The first commonly accepted kinetic model of the 762 nm and 1.27 μm emissions was developed in 1984 (Ref. 4) and significantly refined in 1993 (Ref. 1). Besides the direct excitation of the $O_2(a^1\Delta_g)$ molecules in the ozone photolysis, this model included also the collisional processes of energy transfer from the $O(^1D)$ atoms to the $O_2(b^1\Sigma_g^+)$ molecules and then to the $O_2(a^1\Delta_g)$ molecules. In this model, both the 762 nm and 1.27 μm emissions could equivalently play the role of indicators of the ozone concentration in the atmosphere.

To check the model proposed in Ref. 1, atmospheric experiments on simultaneous measurements of the intensity of both these emissions during daytime were needed.

The first such experiment was conducted by Wallace and Hunten in 1968 (Ref. 5), but its accuracy was insufficient for arriving at conclusions of principle importance.

Another experiment was conducted quite recently.[6] As will be shown below, the vertical ozone profiles retrieved separately from the 1.27-μm and 762-nm emissions with the use of the model from Ref. 1 turn out to differ in the altitude range from 65 to 95 km. Thus, this model fails to provide for unambiguous correspondence between the concentrations of the ozone and the $O_2(a^1\Delta_g)$ and $O_2(b^1\Sigma_g^+)$ molecules.

Unlike the previous kinetic models of $O_2(a^1\Delta_g)$ and $O_2(b^1\Sigma_g^+)$, our analysis takes into consideration the basic facts that, first, photolysis of $O_3$ and $O_2$ and the processes of energy exchange between the photolysis products involve generation of oxygen molecules that are in highly excited vibrational-electronic state and, second, the absorption of solar radiation in the 689 nm and 629 nm bands leads to populating excited vibrational-electronic states $O_2(b^1\Sigma_g^+,\ v = 1)$ and $O_2(b^1\Sigma_g^+,\ v = 2)$, the emission

0235-6880/03/07 536-05 $02.00 

from which is quenched due to collisions down to the level $O_2(b^1\Sigma_g^+, v = 0)$ (Refs. 7 and 8).

As will be shown below, at some altitudes the allowance for the vibrational-electronic kinetics changes the calculated concentrations of the metastable oxygen molecules by 30% and even more.

## 1. New model of 762-nm and 1.27-μm emissions of $O_2$ during daytime

Figure 1 depicts the schematic of chemical processes of formation and loss of the oxygen molecules in singlet metastable states $O_2(a^1\Delta_g)$ and $O_2(b^1\Sigma_g^+)$ that is analyzed in this paper.

The principal novelty of our approach is that the traditional kinetics of the electronically excited products of the $O_3$ and $O_2$ photolysis is supplemented with the processes of energy transfer between the vibrational-electronic excited states of the oxygen molecules $O_2(a^1\Delta_g, v \geq 1)$ and $O_2(b^1\Sigma_g^+, v \geq 1)$ and the oxygen molecules in the ground state $O_2(X^3\Sigma_g^-, v \geq 1)$.

The circles with letters in Fig. 1 are for the following types of the processes taken into account in our model:

*a* – photolysis of $O_2$ in the Schumann–Runge continuum (SRC) in the 120–174 nm region and in the Ly α line:

$$O_2 + \text{photon (SRC, Ly } \alpha) \rightarrow O(^1D) + O(^3P),$$

which are the main sources of $O(^1D)$ atoms above 80 km (Ref. 9);

*b* – photolysis of $O_3$ in the singlet channel (Hartley band at 200–310 nm) (Ref. 10):

$$O_3 + \text{photon (Hartley band)} \rightarrow$$
$$\rightarrow O_2(a^1\Delta_g, v = 0\text{–}5) + O(^1D)$$

and in the triplet channel (Hartley, Higgins, and Chappuis bands in the region from 200 to 600 nm)

$$O_3 + \text{photon (Hartley band)} \rightarrow$$
$$\rightarrow O_2(X^3\Sigma_g^-, v \leq 35) + O(^3P);$$

*c* – EE′-transfer of the electronic excitation energy from the $O(^1D)$ atom to the oxygen molecule[11]:

$$O(^1D) + O_2 \rightarrow O_2(b^1\Sigma_g^+, v \leq 1) + O(^3P);$$

*d* – excitation of $O_2(b^1\Sigma_g^+, v = 1 \text{ and } 2)$ through direct absorption of solar radiation[2,1]:

$$O_2 + \text{photon (762; 689; 629 nm)} \rightarrow$$
$$\rightarrow O_2(b^1\Sigma_g^+, v = 0, 1, 2), \text{ respectively;}$$

*e* – quenching of vibrational excitation of $O_2(b^1\Sigma_g^+, v \geq 1)$ due to intramolecular electronic EE-exchange[8]:

$$O_2(b^1\Sigma_g^+, v \leq 2) + O_2 \rightarrow$$
$$\rightarrow O_2(X^3\Sigma_g^-, v \leq 2) + O_2(b^1\Sigma_g^+, v = 0);$$

a specific feature of this type of reactions is that the electronic level changes in the generated oxygen molecule, while the vibrational quantum number *v* remains unchanged, and such reactions are 2 to 3 orders of magnitude faster than the reactions of inter-level transfer of the electronic excitation energy (reactions of the type *f* in Fig. 1);

*f* – formation of $O_2(a^1\Delta_g, v = 0\text{–}3)$ at collisional quenching of $O_2(b^1\Sigma_g^+, v = 0)$ by the EV type of the exchange[9]:

$$O_2(b^1\Sigma_g^+, v = 0) + M\ (= O_2, N_2, O(^3P), O_3) \rightarrow$$
$$\rightarrow O_2(a^1\Delta_g, v \leq 3) + M;$$

one more channel of excitation of vibrational-electronic $O_2(a^1\Delta_g, v = 0\text{–}5)$ levels is ozone photolysis in the Hartley band, as was noted above;

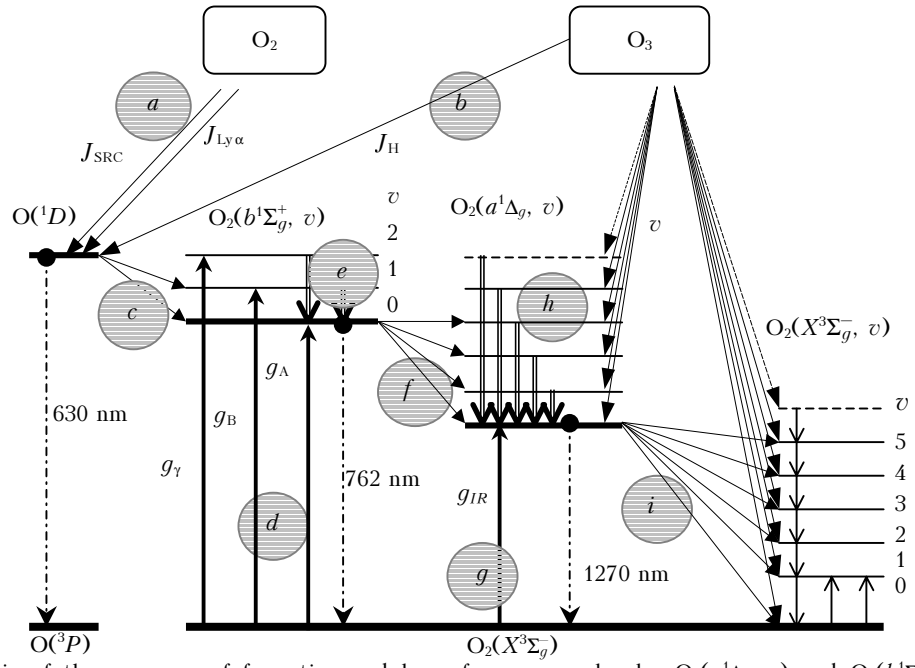


**Fig. 1.** Schematic of the processes of formation and loss of oxygen molecules $O_2(a^1\Delta_g, v)$ and $O_2(b^1\Sigma_g^+, v)$ in the middle atmosphere. The schematic is discussed in Section 1.

$g$ – population of $O_2(a^1\Delta_g, v = 0)$ by absorption of solar radiation[2,1]:

$$O_2 + \text{photon (1.27 μm)} \rightarrow O_2(a^1\Delta_g, v = 0);$$

$h$ – process of EE-quenching of $O_2(a^1\Delta_g, v)$ [Ref. 12] similar to the channel $e$ in Fig. 1:

$$O_2(a^1\Delta_g, v) + O_2(X^3\Sigma_g^-, v = 0) \rightarrow$$
$$\rightarrow O_2(X^3\Sigma_g^-, v) + O_2(a^1\Delta_g, v = 0);$$

$i$ – quenching of $O_2(a^1\Delta_g, v = 0)$ by the type of the EV-exchange[13,14]:

$$O_2(a^1\Delta_g, v = 0) + O_2 \rightarrow$$
$$\rightarrow O_2(X^3\Sigma_g^-, v \le 5) + O_2(X^3\Sigma_g^-, v = 0).$$

The schematic presented in Fig. 1 omits the processes of VT-relaxation of $O_2(a^1\Delta_g, v)$ and $O_2(b^1\Sigma_g^+, v)$ at collisions with $N_2$ and $O(^3P)$ that are taken into account in our calculations. Besides, the so-called Bart mechanism is also omitted in Fig. 1, although taken into account in calculations. This mechanism is based on collisional transfer of energy of the $O_2(\pi)$ precursor generated in the reaction

$$O + O + O_2 \rightarrow O_2(\pi) + O_2$$

to the $O_2(b^1\Sigma_g^+)$ molecule. This channel dominates in nighttime,[15] but in the daytime emission its contribution, according to our calculations, does not exceed 2.5% nearby the peak (about 96–100 km) of the atomic oxygen concentration. Totally more than 100 reactions are included in the model.

## 2. Calculation of $O_2(a^1\Delta_g, v = 0)$ and $O_2(b^1\Sigma_g^+, v = 0)$ concentrations in the middle atmosphere

The model proposed was used to calculate the concentrations of $O_2(a^1\Delta_g, v = 0)$ and $O_2(b^1\Sigma_g^+, v = 0)$ and, correspondingly, the intensity of the 1.27-μm and 762-nm emissions in the middle atmosphere. Figure 2 compares the experimental data[6] on the vertical profile of the rate of volume emission at the wavelength of 762 nm and the calculations for the experimental conditions provided by our model and the model from Ref. 1. In our calculations we used the MSISE90 model of the atmosphere.

One can see that our results calculated for $[O_2(b^1\Sigma_g^+, v = 0)]$ differ from the values given by the model from Ref. 1 at heights above 100 km and below 40 km. Figure 2 presents the relative deviations of the rate of volume emission at 762 nm between our calculations and the values given by the model from Ref. 1. Above 40 km the dominating process is the transfer of the electronic excitation energy from the $O(^1D)$ atom to the $O_2(b^1\Sigma_g^+, v = 0, 1)$ molecule (process $c$ in Section 1). In Ref. 1 it was assumed that in this reaction all molecules are formed in the state $O_2(b^1\Sigma_g^+, v = 0)$ with the quantum yield of 0.77. However, according to the current ideas, the quantum yield of $O_2(b^1\Sigma_g^+, v = 0)$ in this reaction is only 0.45, while the quantum yield of $O_2(b^1\Sigma_g^+, v = 1)$ is equal to 0.32 (Ref. 11). As a result, above 100 km the model from Ref. 1 gives 20-30% overestimated results of the rate of volume emission at 762 nm as compared with our calculations. At the altitudes below 35 km, the excitation of $O_2(b^1\Sigma_g^+, v = 1)$ at absorption of solar radiation (process $d$, Section 1), which was ignored in Ref. 1, is responsible for more than 20% of the rate of $O_2(b^1\Sigma_g^+, v = 0)$ formation.

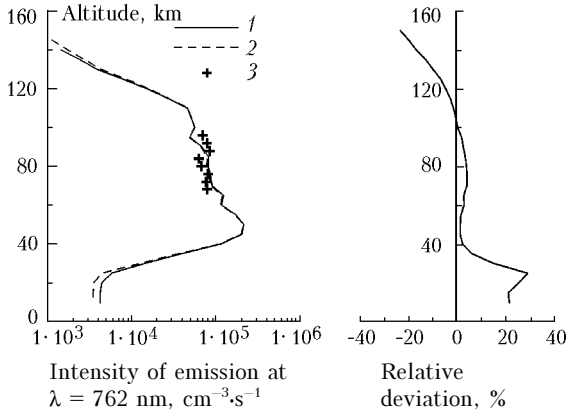


**Fig. 2.** Rate of volume emission at 762 nm for $O_2(b^1\Sigma_g^+, v = 0)$ (left): our model (*1*) and model from Ref. 1 (*2*), experiment[6] (*3*). Deviation of calculation by our model from calculation by the model from Ref. 1 (right).

In the same experiment, in Ref. 6, the intensity of the 1.27-μm emission was measured simultaneously. Figure 3 compares the $O_2(a^1\Delta_g, v = 0)$ concentration profiles calculated by our model and the model from Ref. 1 with the experiment from Ref. 6 and the measurements and calculations by other authors.

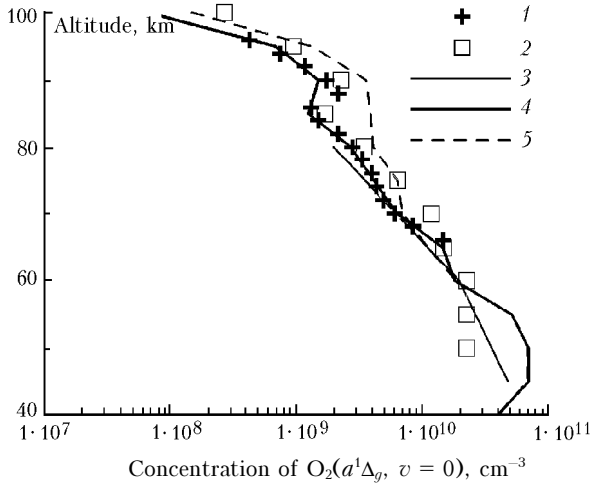


**Fig. 3.** Concentration of $O_2(a^1\Delta_g, v = 0)$ molecules; experiment from Ref. 6 (*1*) and from Ref. 4 (*2*); calculation of Ref. 16 (*3*), our model (*4*), model of Ref. 1 (*5*).

As can be seen, our calculations agree well with the experimental data and even predict the second peak of the IR Atm $O_2$ emission in the range of 85–95 km. In the altitude range of 65–90 km, our calculations $[O_2(a^1\Delta_g, v = 0)]$ are 30–40% lower than

similar results calculated by the model from Ref. 1 and far closer to the measured values.

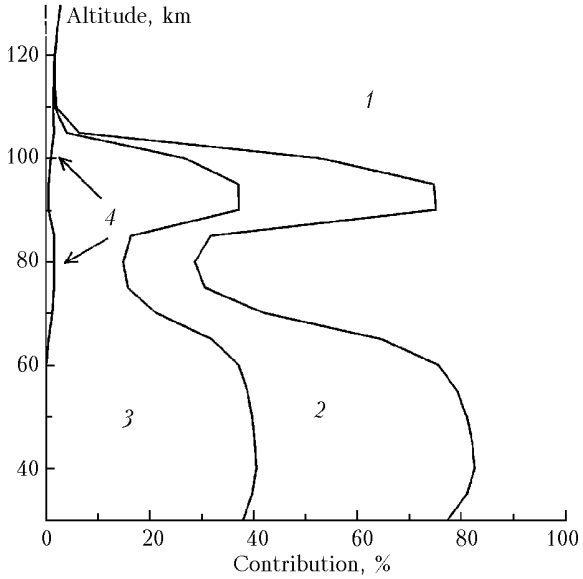


**Fig. 4.** Relative contribution of different channels to the total rate of $O_2(a^1\Delta_g,\ v = 0)$ production, in percent: energy transfer $O(^1D) \rightarrow O_2(b^1\Sigma_g^+,\ v) \rightarrow O_2(a^1\Delta_g,\ v = 0)$ (*1*), ozone photolysis in the Hartley band $O_3 \rightarrow O_2(a^1\Delta_g,\ v \geq 1) \rightarrow O_2(a^1\Delta_g,\ v = 0)$ (*2*), ozone photolysis in the Hartley band $O_3 \rightarrow O_2(a^1\Delta_g,\ v = 0)$ (*3*), absorption of solar radiation $O_2$ + photon (1.27 μm) $\rightarrow O_2(a^1\Delta_g,\ v = 0)$ (*4*).

Consider relative contributions of different channels to formation of $O_2(a^1\Delta_g,\ v = 0)$ (Fig. 4). Below 60 km the dominating process is the ozone photolysis due to absorption within the Hartley band (channels *2* and *3* in Fig. 4). Above 60 km the dominating process is the electronic excitation energy transfer from the $O(^1D)$ atom to the $O_2(b^1\Sigma_g^+,\ v = 0, 1)$ molecule and then to the $O_2(a^1\Delta_g,\ v = 0)$ molecule (channel *1* in Fig. 4). The local peak of the rate of $O_2(a^1\Delta_g,\ v = 0)$ formation in the range of 85–95 km is associated with the fast reaction of VT-quenching at collisions with the atomic oxygen

$$O_2(a^1\Delta_g,\ v) + O(^3P) \rightarrow O_2(a^1\Delta_g,\ v = 0) + O(^3P)$$

with the rate constant of about $10^{-11}$ $cm^3 \cdot s^{-1}$ (Ref. 12).

Thus, the observed local peak $[O_2(a^1\Delta_g,\ v = 0)]$ at the altitudes of about 90 km is associated not only with the corresponding local ozone peak, but also with the above processes of vibrational-electronic relaxation.

## 3. Retrieval of the vertical ozone profile from the measured emission intensity profiles at 762 nm and 1.27 μm

The validity of our kinetic model of vibrational-electronic relaxation of the $O_3$ and $O_2$ photolysis products can be checked through interpretation of the atmospheric experiment on retrieval of the vertical ozone profile from simultaneous records of the intensity in the Atm and IR Atm bands of the $O_2$ molecule.[6] Using our model and the model from Ref. 1, we have solved the inverse problem of $[O_3]$ determination from measurements of the 762-nm and 1.27-μm emissions. Figure 5 depicts the results of retrieval of the ozone concentration.

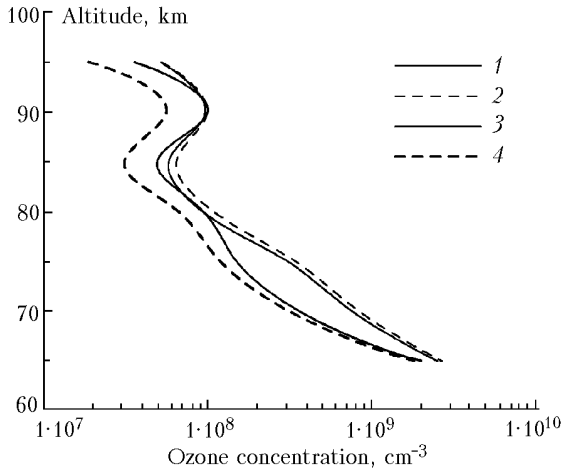


**Fig. 5.** Vertical ozone profile retrieved from observation of emission at 762 nm: our model (*1*) and model from Ref. 1 (*2*), and from emission at 1.27 μm: our model (*3*) and model from Ref. 1 (*4*).

In analyzing the retrieved ozone profiles, two altitude ranges, below and above 78 km, should be separated. This is connected with the fact that, as was noted in Ref. 6 (whose experimental results are considered in this paper) below 78 km their experimental data on the intensities of the 762 nm and 1.27 μm emissions included a systematic error leading to the difference between the retrieved ozone profiles. Similar conclusion follows from our model for this altitude range as well.

However, above 78 km, according to our model, as was already mentioned above, the vibrational-electronic kinetics of the products of $O_3$ and $O_2$ photolysis begins to play a significant role in the mechanism of formation of these emissions. As a result, above 78 km the retrievals of $[O_3]$ by our model and the model of Ref. 1 differ significantly.

### a) Model from Ref. 1

In the region of the local peak of $[O_3]$ near 90 km, the $O_3$ concentration retrieved from the intensity of the IR Atm $O_2$ band is almost halved as compared to that retrieved from the intensity of the Atm $O_2$ band (see dashed lines in Fig. 5).

### b) Our model

The vertical $[O_3]$ profiles retrieved from both of the emissions agree with each other, and in the

altitude range of 80–95 km the mean discrepancy is within 6%. The $[O_3]$ value retrieved by our model in the range of a local peak is almost twice as large as that obtained by the model from Ref. 1 from the intensity of the 1.27-μm IR Atm bands of the $O_2$ molecule (solid lines in Fig. 5).

In other words, the use of previous model of the daytime 1.27-μm emission from Ref. 1 in retrieving the vertical ozone profile underestimates the $[O_3]$ value almost two times in the altitude range of 85–95 km.

## Conclusions

1. We have developed the model of kinetics of the excited products of the ozone and oxygen photolysis, which takes into account the processes of energy transfer between vibrational-electronic excited states of the oxygen molecule $O_2(a^1\Delta_g, v)$ and $O_2(b^1\Sigma_g^+, v)$, excited oxygen atoms $O(^1D)$, and oxygen molecules in the ground state $O_2(X^3\Sigma_g^-, v)$.

2. The model proposed allows calculation of not only vertical profiles of the $O_2(a^1\Delta_g, v = 0)$ and $O_2(b^1\Sigma_g^+, v = 0)$ concentrations, but also the profiles of $[O_2(a^1\Delta_g, v \le 5)]$ and $[O_2(b^1\Sigma_g^+, v = 0, 1, 2)]$.

3. With the allowance made for the vibrational-electronic kinetics of the excited products of the ozone and oxygen photolysis, the altitude profiles retrieved from the measured intensities of the 762-nm and 1.27-μm emissions agree with each other.

### Acknowledgments

The authors are grateful for information support and useful discussions to their colleagues: V.I. Fomichev (York University, Canada), T.G. Slanger (SRI International, Menlo Park, California), and A.O. Semenov (St. Petersburg University).

The support from the Russian Foundation for Basic Research (Grants No. 02–05–65259 and No. 00–05–65082) is acknowledged.

### References

1. M.G. Mlynczak, S.C. Solomon, and D.S. Zaras, J. Geophys. Res. **98**, No. D10, 18639–18648 (1993).
2. A. Bucholtz, W.R. Skinner, V.J. Abreu, and P.B. Hays, Planet. Space Sci. **34**, No. 11, 1031–1035 (1986).
3. M.G. Mlynczak and B.T. Marshall, Geophys. Res. Lett. **23**, No. 6, 657–660 (1996).
4. R.J. Thomas, C.A. Barth, D.W. Rusch, and R.W. Sanders, J. Geophys. Res. **89**, No. D6, 9569–9580 (1984).
5. A.D. Danilov and M.N. Vlasov, *Photochemistry of Ionized and Excited Particles in the Lower Ionosphere* (Gidrometeoizdat, Leningrad, 1973), 190 pp.
6. M.G. Mlynczak, F. Morgan, J.-H. Yee, P. Espy, D. Murtagh, B.T. Marshall, and F. Schmidlin, Geophys. Res. Lett. **28**, No. 6, 999–1002 (2001).
7. H.I. Bloemink, R.A. Copeland, and T.G. Slanger, J. Chem. Phys. **109**, No. 11, 4237–4245 (1998).
8. K.S. Kalogerakis, R.A. Copeland, and T.G. Slanger, J. Chem. Phys. **116**, No. 12, 4877–4885 (2002).
9. W.B. DeMore, D.M. Golden, R.F. Hampson, C.J. Howard, C.E. Kolb, and M.J. Molina, "*Chemical kinetics and photochemical data for use in stratospheric modeling*," JPL Publication, Vol. 97–4. Evaluation Number 12, pp. 1–128 (1997).
10. M.-A. Thelen, T. Gejo, J.A. Harrison, and J.R. Huber, J. Chem. Phys. **103**, No. 18, 7946–7955 (1995).
11. D.L. Baulch, R.A. Cox, P.J. Crutzen, R.F. Hampson, Jr, J.A. Kerr, J. Troe, and R.T. Watson, J. Phys. Chem. Ref. Data **11**, No. 2, 327–496 (1982).
12. T.G. Slanger, Private communication (to be published in J. Chem. Phys. 2003).
13. E. Wild, H. Klingshirn, B. Faltermeier, and M. Maier, Chem. Phys. Lett. **93**, No. 5, 490–494 (1982).
14. J.G. Parker, J. Chem. Phys. **67**, No. 11, 5352–5361 (1977).
15. D.P. Murtagh, G. Witt, J. Stegman, I.C. McDade, E.J. Llewellyn, F. Harris, and R.G.H. Greer, Planet. Space Sci. **38**, No. 1, 43–53 (1990).
16. T. Shimazaki, J. Atmos. Terr. Phys. **46**, No. 2, 173–191 (1984).